General Disclaimer

One or more of the Following Statements may affect this Document

- This document has been reproduced from the best copy furnished by the organizational source. It is being released in the interest of making available as much information as possible.

- This document may contain data, which exceeds the sheet parameters. It was furnished in this condition by the organizational source and is the best copy available.

- This document may contain tone-on-tone or color graphs, charts and/or pictures, which have been reproduced in black and white.

- This document is paginated as submitted by the original source.

- Portions of this document are not fully legible due to the historical nature of some of the material. However, it is the best reproduction available from the original submission.

RADIANT HEAT EXCHANGE IN A SPACE ENVIRONMENT

Research and Development Contract No. 951661
California Institute of Technology
Jet Propulsion Laboratory
4800 Oak Grove Drive
Pasadena, California

University of Illinois Budget Code: 46-22-40-352

Scientific Technical Report No. 6

Period Covered: August 1, 1969, to January 31, 1970

Prepared by: R. G. Hering
T. F. Smith
W. D. Fischer

Submitted by: R. G. Hering
Professor of Mechanical Engineering
266 Mechanical Engineering Building
University of Illinois at Urbana-Champaign
Urbana, Illinois 61801
Phone: Area Code 217, 333-0366

Date: January 31, 1970

TABLE OF CONTENTS

This work was performed for the Jet Propulsion Laboratory, California Institute of Technology, sponsored by the National Aeronautics and Space Administration under Contract NAS7-100.

1. OBJECTIVES AND SCOPE

Studies are being conducted to develop analytical methods for predicting radiant heat transfer and temperature of engineering surfaces in a space environment. These studies include two major aspects. First, by thoroughly investigating the influence of directional and spectral property dependencies of engineering materials on radiant heat transfer and temperature by means of detailed analysis, the accuracy of present calculation methods may be assessed, new and improved methods developed, and the surface property data required to implement the new methods delineated. Second, since the results of analysis are only as valid as the surface property models employed, a facility is under development to measure bidirectional reflectance of surfaces with the aim of justifying and refining a bidirectional reflectance model for metallic engineering surfaces.

In Section 2 the progress made during a sixth six-month period of the contract is summarized and the current status of the research program reviewed. The anticipated progress for the next six-month period is discussed in Section 3.

2. CURRENT STATUS

The progress made and current status of the research program are reviewed under three major categories. Advances in the theoretical heat transfer effort are reported in Section 2.1. Section 2.2 is devoted to analytical efforts to establish realistic radiation property models for engineering surfaces. The progress in the development of a bidirectional reflectance measurement facility is reviewed in Section 2.3.

2.1 RADIANT HEAT TRANSFER ANALYSIS

2.1.1 Radiant Heat Transfer for Non-gray, Non-diffuse Surfaces in a Space Environment

Calculations which account for real surface property effects on radiant heat transfer and equilibrium temperature for interacting surfaces in a space environment have been completed. The results are being compared to calculations employing simple surface property models for radiative transfer. The comparison is providing a means for assessing the extent to which present design techniques account for real surface effects and estimates of the magnitude of the error in heat flux and equilibrium temperature incurred by the use of simple property models. The real surface calculations also point out the level of radiation surface property detail required in radiant heat transfer calculations to assure acceptable design accuracy and delineate the surface property measurements necessary to implement improved thermal design methods.

Numerical results for radiant heat transfer in the absence of a solar flux and for equilibrium temperature of radiatively adiabatic surfaces in a solar field have been evaluated. Similar results have been obtained for simple surface property models and compromise models which attempt to retain the computational simplicity of simple models, yet partially account for important real surface characteristics. The details of the calculations and the resulting conclusions are the subject of a forthcoming report. Upon completion, this report will be submitted under separate cover.

2.1.2 Radiant Heat Transfer and Equilibrium Temperature of Surfaces with One-dimensional Roughness

Apparent thermal radiation properties for surfaces with one-dimensional V-groove roughness elements have been developed [1, 2,3]†. These properties were derived employing concepts of geometrical optics and apply for optical roughness values in excess of unity. Analysis is underway to utilize the apparent properties to study the influence of directional emission and reflection on heat transfer and on equilibrium temperature of surfaces in a space environment. Studies are in various stages of completion for both isolated surfaces and systems of radiatively interacting surfaces. These studies complement those cited in Section 2.1.1 which employ a bidirectional reflectance model appropriate to surfaces with small optical roughness.

†Numbers in brackets refer to entries in REFERENCES.

2.1.2.1 Isolated Surfaces

In an earlier report [2], preliminary results illustrating the influence of surface roughness on heat transfer and on the temperature acquired by an isolated radiatively adiabatic surface in a solar flux were presented. Two manuscripts were prepared and subsequently published [4,5]. Since details are available in the articles, emphasis is given here to the presentation of typical results and the conclusions drawn from these studies.

The ratio of equilibrium temperature of a rough surface, T_R, to equilibrium temperature of a smooth surface of identical constituent material, T_S, is illustrated in Fig. 1 as a function of dimensionless direction of incident energy $\theta'/(\chi/2)$. Typical apparent properties of the rough surface are illustrated in the insert for material emittance (ε_w) and solar absorptance (α_w^*) values of 0.1 and 0.9. The results of Fig. 1, as well as others [4], demonstrate that large errors in equilibrium temperature can result if the influence of surface roughness on thermal radiation properties is ignored. Complete neglect of surface roughness yields temperatures which vary from 34 percent lower to 18 percent higher than those acquired by the rough surface. Surface roughness effects are particularly important for surfaces with small and large values of α_w^*/ε_w. The dependence of equilibrium temperature on direction of incident energy is particularly severe for surfaces of low solar absorptance and, for the most part, negligible for surfaces of high solar absorptance.

Dimensionless radiant heat transfer, $q/\sigma T^4$, from a rough surface with apparent emittance ϵ_H and direction dependent apparent solar absorptance $\alpha_a^*(\theta')$ in a solar field of solar constant S is presented in Fig. 2 for material property values 0.1 and 0.9. The parameter S^* ($= S/\sigma T^4$) is a dimensionless energy ratio characterizing the relative magnitude of solar flux to surface emission rate. Results illustrated in Fig. 2 demonstrate that surface roughness can significantly influence radiant heat transfer rates. When roughness is completely neglected and fluxes are evaluated using material property values, the discrepancy between values so calculated and those which fully account for roughness can be orders of magnitude when the dimensionless fluxes are less than unity. For dimensionless flux values greater in absolute value than unity, the difference exceeds 10 percent. Surface roughness effects are particularly important for low emittance surfaces when emission is dominant, low solar absorptance materials when incident flux is dominant, and for materials with α_w^*/ϵ_w near unity in situations where emission rate and incident flux are comparable. The use of apparent emittance and normal solar absorptance for all directions of incident energy yields results in excellent agreement with rough surface fluxes except for materials of low solar absorptance in solar flux dominated situations at intermediate directions of incidence.

2.1.2.2 Interacting Surfaces

Analysis and numerical results have been completed describing the influence of one-dimensional surface roughness on

radiant heat transfer for interacting surfaces in the absence of external radiation fields. Two simple systems of surfaces were selected for study. Results for the adjoint plate system were summarized in an earlier report [6]. A manuscript was prepared describing the details of the analysis and results [7] and was recently accepted for publication in a technical journal. Reprints of the article will be submitted to JPL upon receipt. Results for the parallel plate system illustrated in Fig. 3 were also obtained and a manuscript based on this study was recently accepted for publication [8]. Typical results and a short summary of important conclusions from this study are presented next.

Dimensionless radiant heat flux distributions evaluated from the rough surface analysis, as well as from the less detailed analysis required for simpler property models, are illustrated in Fig. 4 for a low emittance material and selected values for the spacing parameter h/ℓ. Results obtained using the diffuse emission-diffuse reflection model which ignores directional dependence of properties are denoted CD (constant diffuse). If reflection is considered specular, the corresponding results are denoted CS (constant specular). Radiant flux distributions were obtained for the direction independent property models employing hemispherical emittance values ε_H given by rough surface material emittance ε_w and rough surface apparent emittance ε_a. Constant property results based on wall emittance completely neglect the influence of roughness on surface properties and, hence, heat transfer. Constant property results obtained

using apparent emittance account for the influence of surface roughness on the magnitude of energy emission and reflection, but disregard roughness influences on the spatial distribution of emitted and reflected energy.

Consider first the results for small spacing. At the plate edge CD analyses using wall emittance yield fluxes which are low by 24 percent for a surface with specularly reflecting asperities of small slope and by a factor of two for a surface with diffusely reflecting elements of large slope. CS analysis with ε_w is even poorer. As x/ℓ increases, the constant property model flux results approach, intersect, and, finally, exceed rough surface fluxes at the plate center where CD results are high by 40 percent. CS results are even less accurate near the plate center. Flux distributions valuated with diffuse analysis and apparent hemispherical emittance most closely approximate those of the rough surfaces. Although CD analysis with ε_a reduces the edge flux error to an acceptable level (maximum 10 percent), no significant improvement occurs at the plate center. For intermediate h/ℓ values, the rough surface flux distributions generally are intermediate to those calculated with diffuse analysis using wall emittance and apparent emittance. While diffuse analysis with apparent emittance appears to yield the best approximation to the flux results for surfaces with diffusely reflecting roughness elements, neither diffuse nor specular analysis adequately approximates the flux distribution for surfaces with specularly reflecting elements, particularly for the surface with larger roughness

slope. For $h/\ell = 1.0$, CD analysis with ε_a yields results which differ imperceptibly from those for the surface with diffuse elements and 90° included angle. Agreement is acceptable for the surface with diffuse elements of the smaller included angle also. Again, however, the rough surface flux distribution for specularly reflecting roughness elements is poorly represented by the results of constant property analysis. The trends observed for $\varepsilon_w = 0.1$ are evident, but to a lesser degree for the intermediate wall emittance surface. Diffuse analysis with roug' surface apparent hemispherical emittance yields flux distributions in good agreement with rough surface results throughout the entire range of values for the spacing parameter when wall emittance is large.

The following conclusions may be drawn from the radiant heat transfer results. Surface roughness effects are relatively unimportant for high emittance materials ($\varepsilon_w \geq 0.9$). The influence of surface roughness on radiant transfer steadily increases as material emittance values diminish. Surface roughness slope is the more dominant rough surface parameter influencing radiant transfer. For low emittance materials surface roughness can alter local flux by 50 percent and total heat transfer by a factor of two. Comparison of rough surface heat flux distributions to those evaluated with simple surface property models demonstrated that neither diffuse nor specular analysis can consistently approximate the rough surface results over the range of values considered for the radiant interaction parameter h/ℓ. Overall, diffuse analysis with rough surface

10

apparent emittance gave the better representation although local flux discrepancies as large as 50 percent and more were not uncommon. Rough surface total heat transfer was accurately predicted (within 3 percent) by diffuse analysis employing rough surface apparent emittance. This excellent agreement deteriorated rapidly as material emittance decreased.

The analyses briefly described above have been extended to include evaluation of local and overall radiant interchange factors. These factors are important for calculation of net radiant energy transfer between interacting surfaces and for describing radiant transfer between surfaces when other energy transfer modes, such as conduction and convection, are present. Computations have been completed, but the results require further study.

Analysis was completed which extends that developed for the adjoint plate system to include solar flux and, hence, evaluation of surface roughness effects on equilibrium temperature of radiatively adiabatic interacting surfaces. Numerical results are being obtained, but are not yet sufficient in quantity to report any conclusions.

2.1.3 Spectral Surface Property Effects on Radiant Transfer

An analysis has been completed which provides a mechanism for study of spectral surface property effects on radiant heat transfer between radiatively interacting surfaces. The system of surfaces initially chosen for study is the adjoint plate system in the absence of external thermal radiation fields. One of the purposes

of this analysis is to provide information which can be utilized to delineate the relative importance of spectral and directional real surface property dependencies. Furthermore, additional information is required to ascertain the magnitude of the error incurred in gray and semigray methods of analysis.

Numerical results were recently acquired for identical uniform property adjoint plates. Roberts' expressions [9] were employed to describe the wavelength dependence of the optical parameters in the relations of electromagnetic theory for hemispherical emittance [10]. Initial study was restricted to tungsten for which Roberts reported values of the empirical constants which gave good agreement with spectral hemispherical emittance data. Dimensionless radiant flux distributions are illustrated in Fig. 5 for equal temperature diffuse tungsten surfaces at a temperature of 1980°R. Differences between local gray and nongray heat flux values are of the order of 5 percent and are a weak function of location on the surfaces. As a consequence of the last observation, most trends related to spectral dependence of properties may be studied by comparing gray and nongray heat flux values at a selected location on the surfaces. The common edge ($x/L = 0$) is convenient because the spectral heat flux may be evaluated from analytical expressions for diffusely emitting surfaces described by a direction independent specular-diffuse reflection model.

Dimensionless corner heat flux values, $q(0)/\sigma T^4$, evaluated from nongray and gray analyses are compared in Fig. 6 for equal temperature

plates. Results are shown for diffusely reflecting surfaces ($\rho^s/\rho = 0.0$), specularly reflecting surfaces ($\rho^s/\rho = 1.0$), and surfaces of intermediate specularity ($\rho^s/\rho = 0.5$) over a large temperature range. Corner flux values evaluated with the gray spectral model are in error by a maximum of approximately 6 percent at intermediate temperatures of 2000-3000°R. The magnitude of the error in gray results is relatively independent of the reflection model.

For the material and temperature range considered, the difference between corner heat flux values calculated on the basis of a gray and nongray spectral model for properties is small. Branstetter [11] also reported relatively small differences for parallel tungsten plates when the difference in temperature between the plates was small. When large temperature differences were involved, however, Branstetter observed large discrepancies in gray and nongray radiant transfer rates. The analysis for the adjoint plate system was extended to unequal temperature plates in order to investigate whether a similar observation could be made for this system. Typical corner heat flux results are presented in Fig. 7 for the adjoint plate system with the higher temperature plate at a temperature of 4320°R. The temperature of the adjacent surface was varied from 536°R to the temperature value of the hotter surface. In agreement with Branstetter's findings, the results of Fig. 7 establish that the gray spectral property model gives poorer agreement with nongray analysis as the temperature difference between the surfaces increases. It may also be noted that the lower temperature plate is more sensitive to the spectral dependence of properties.

The analyses and results briefly discussed in this section are being extended to include other materials and spectral property models. Other extensions of the analyses under consideration include studies which account for both spectral and directional property dependence as well as influences of spectral property dependence on equilibrium temperature.

2.2 RADIATION PROPERTY ANALYSIS

The study of apparent radiation properties of surfaces with one-dimensional roughness elements [3] which was presented at the AIAA Fourth Thermophysics Conference will be published in the AIAA Series, Progress in Astronautics and Aeronautics: Thermophysics--Application to Thermal Design of Spacecraft. Reprints of the article will be submitted to JPL upon receipt.

2.3 BIDIRECTIONAL REFLECTANCE MEASUREMENT FACILITY

Plane of incidence bidirectional reflectance measurements previously reported [6] indicated that certain modifications to the facility were necessary. The modifications initiated are designed to

(1) eliminate an erratic reference signal from the monochromator chopper assembly,

(2) reduce mirror alignment and wavelength-drum calibration difficulties of the system,

(3) extend capability to continuous angle scanning, and

(4) implement automatic acquisition and reduction of reflectance data.

The design changes are in various stages of completion and are discussed in the remainder of this section.

Problems attributed to the erratic reference signal from the internal chopper of the monochromator were eliminated by two design modifications. First, the chopper motor supplied with the monochromator was replaced with a synchronous motor and the driver pulley was redesigned so that the chopper and amplifier operate at the same frequency. Second, the mechanical cam system of the monochromator which furnishes a reference signal to the amplifier was replaced with a photodiode system. The redesigned reference signal unit consists of a stationary narrow light beam, a semicircular blade attached to the chopper shaft, and a stationary photodiode. As the shaft rotates, the blade interrupts the light beam which is focused on the photodiode. The photodiode transforms the alternating light beam signal to an alternating electrical voltage signal which triggers the amplifier. The above design modifications have been completed and the erratic reference signal eliminated so that now the amplifier is able to lock-on to the reference signal.

Design modifications were initiated to reduce the difficulty in calibration of the monochromator wavelength drum drive. A 200 step per revolution stepping motor purchased from Superior Electric Company was attached to the wavelength drum shaft. One step of the motor corresponds to 0.005 drum divisions. A two axis indexer acquired from the same vendor drives this motor, as well as the angle scan motor discussed below. These design changes have been completed

and subsequent use of the equipment has demonstrated significant reduction in the time required for wavelength drum calibration, as well as substantial improvement in repeatability and accuracy of drum calibration.

Alignment of illuminating and detecting optics of the reflectance facility has been a particularly difficult procedure. As a result, the illuminating and detecting optical systems have been modified to that schematically illustrated in Figs. 8 and 9. As with the original design [2], the illuminating optical system consists of a radiant energy source, a plane mirror, and a spherical mirror. Supports for these components were redesigned to reduce alignment difficulties. All supports are attached to the source arm. In order to provide capability for continuous scanning over the direction of reflected energy (θ angle in Fig. 8), the detecting optical system is suspended from an arm rigidly attached to the monochromator. The optics consists of two plane mirrors and a spherical mirror which is interchangeable with other spherical mirrors. Supports for these mirrors are positioned so that interference with the illuminating optics supports is eliminated as the source arm is rotated. Six spherical mirrors were purchased and these enable selection of 0.001535, 0.00307, or 0.00614 steradian solid angle for study of the influence of solid angle size on measurements. The angles of incidence (θ') and reflection (θ) are set by the use of the rotary table assembly [2]. Direction of incident energy on the sample is manually adjusted with the upper rotary table. A 200 step per revolution stepping

motor recently purchased is employed to scan over direction of reflected energy by driving the lower rotary table through a speed reducer. One step of the motor is equivalent to 0.01 degree change in the direction of reflected energy. The indexer previously mentioned drives the stepping motor for angle scan. Although all redesign has been completed, not all components have been constructed.

A Hewlett-Packard Model 2012B digital data acquisition system with magnetic tape recorder was recently received on a loan basis from JPL. The system was subsequently checked out by qualified personnel from the vendor. Since the available IBM 360 computer facility requires a nine track tape, the seven track tape of the digital data acquisition system must be translated from the seven track to nine track tape before computer processing of data can be accomplished. Procedures have been developed to effect this translation. A computer code converts the translated data on the nine track tape to a format compatible with the available computing facility. This code has been written and verified. Additional features incorporated into the data reduction code include the storage of converted data onto a disk file from which it can be operated on or plotted.

Since the indexer for scanning over wavelength and direction of reflected energy and the data acquisition system are independent units, it was necessary to design an interface between these systems. A schematic diagram of the interface control system is illustrated in Fig. 10. The system designed† uses integrated circuits, but

†The assistance of Professor W. E. Bair, Department of Mechanical and Industrial Engineering, University of Illinois at Urbana-Champaign, in designing the circuitry is gratefully acknowledged.

otherwise standard electrical components. Although component layout has not been finalized, the operational characteristics of the system have been formulated. The control system consists of a recorder control, wavelength drive control, and angle scan control. The recorder includes a start circuit, amplifier response delay circuit, encoder, and background measurement control circuit. The delay circuit is designed so that a pulse at A or B (see Fig. 10) is delayed for a time interval directly related to amplifier response. This provision enables the amplifier to fully respond to a change in level of the voltage signal from the detector. The encoder has been designed to include the capability of recording amplifier voltage signal with the data acquisition system up to ten times. This feature provides a mechanism for averaging the signal when noise levels are high. Upon completion of the encoding operation, a pulse is given to the background unit where a switch has been incorporated to distinguish whether a background signal is to be recorded or the unit is to be bypassed. In the background mode of operation, a pulse is available at S to trigger a shutter which eliminates sample illumination by the radiation source. Simultaneously, a pulse to B triggers the amplifier delay unit. After having recorded the background signal, a pulse is provided at C. This pulse is transferred to either the wavelength drive control unit or the angle scan control unit depending on the setting of the function switch. In either unit, a counter and corresponding stepper motor are then activated and either the wavelength or angle of reflection is incremented

the desired number of steps. After incrementing, a pulse is available at B to repeat the process which is then continued until measurements have been acquired over the entire range of wavelength and/or angle of reflection. The circuitry for the interface system has been developed and is under construction.

3. FUTURE RESEARCH

Future efforts in theoretical studies will concentrate first on the completion of the real surface radiant transfer study utilizing the detailed bidirectional reflectance models. Details of the analysis, quantitative results, and the important conclusions drawn from this study are being documented in an extensive report devoted entirely to this investigation. This report is nearing completion and will be submitted shortly.

Theoretical studies of surface roughness effects on radiant heat transfer and equilibrium temperature of grooved surfaces will continue. Computations of real surface local and overall radiant interchange factors for both the adjoint plate system and the parallel plate system are nearing completion and will delineate the influence of surface roughness on radiant interchange for systems of surfaces of widely different character. Subsidiary analyses and computations are underway to investigate the accuracy of simple reflection models in predicting real surface radiant transfer. Results are also being realized for the extended real surface analysis which includes solar flux. This study will permit evaluation of surface roughness effects on equilibrium temperature distribution. All the above cited efforts are expected to be completed within the next six-month contract period. Studies of the influence of spectral dependence of surface properties on radiant heat transfer and equilibrium temperature will be continued.

Upgrading of the bidirectional reflectance facility to (1) automatically scan over all directions of reflected energy in the plane of incidence, (2) automatically scan over the wavelength region of interest, and (3) fully utilize the capabilities of the data acquisition system is expected to be completed shortly. Bidirectional reflectance measurements in the plane of incidence for surfaces with well-defined characteristics, as well as other selected samples, will commence upon completion of system improvements.

4. REFERENCES

1. Hering, R. G., Houchens, A. F., Smith, T. F., Fischer, W. D., and Hill, G., "Radiant Heat Exchange in a Space Environment," Scientific Technical Report No. 2, Contract No. 951661, Jet Propulsion Laboratory, California Institute of Technology (1967).

2. Hering, R. G., Houchens, A. F., Smith, T. F., and Fischer, W. D., "Radiant Heat Exchange in a Space Environment," Scientific Technical Report No. 3, Contract No. 951661, Jet Propulsion Laboratory, California Institute of Technology (1968).

3. Hering, R. G., and Smith, T. F., "Apparent Radiation Properties of a Rough Surface," AIAA No. 69-622, to be published in AIAA Series Progress in Astronautics and Aeronautics: Thermophysics--Applications to Thermal Design of Spacecraft.

4. Hering, R. G., and Smith, T. F., "Surface Roughness Effects on Equilibrium Temperature," Journal of Spacecraft and Rockets, Vol. 6, No. 8, p. 955 (August 1969).

5. Hering, R. G., and Smith, T. F., "Surface Roughness Effects on Radiant Heat Transfer," Journal of Spacecraft and Rockets, Vol. 6, No. 12, p. 1465 (December 1969).

6. Hering, R. G., Houchens, A. F., Smith, T. F., and Fischer, W. D., "Radiant Heat Exchange in a Space Environment," Scientific Technical Report No. 5, Contract No. 951661, Jet Propulsion Laboratory, California Institute of Technology (1969).

7. Hering, R. G., and Smith, T. F., "Surface Roughness Effects on Radiant Transfer between Surfaces," to be published in International Journal of Heat and Mass Transfer.

8. Hering, R. G., Smith, T. F., and Shaffer, J. T., "Surface Roughness Effects on Radiant Transfer between Surfaces," accepted for presentation and publication in Proc. Fourth Int. Heat Transfer Conference, Paris, France (1970).

9. Roberts, S., "Optical Properties of Nickel and Tungsten and Their Interpretation According to Drude's Formula," Physical Review, Vol. 114, No. 1 (1959).

10. Hering, R. G., and Smith, T. F., "Surface Radiation Properties from Electromagnetic Theory," International Journal of Heat and Mass Transfer, Vol. 11, p. 1567 (1968).

11. Branstetter, J. R., "Radiant Heat Transfer between Nongray Parallel Plates of Tungsten," NASA TN D-1088 (1961).

5. FIGURES

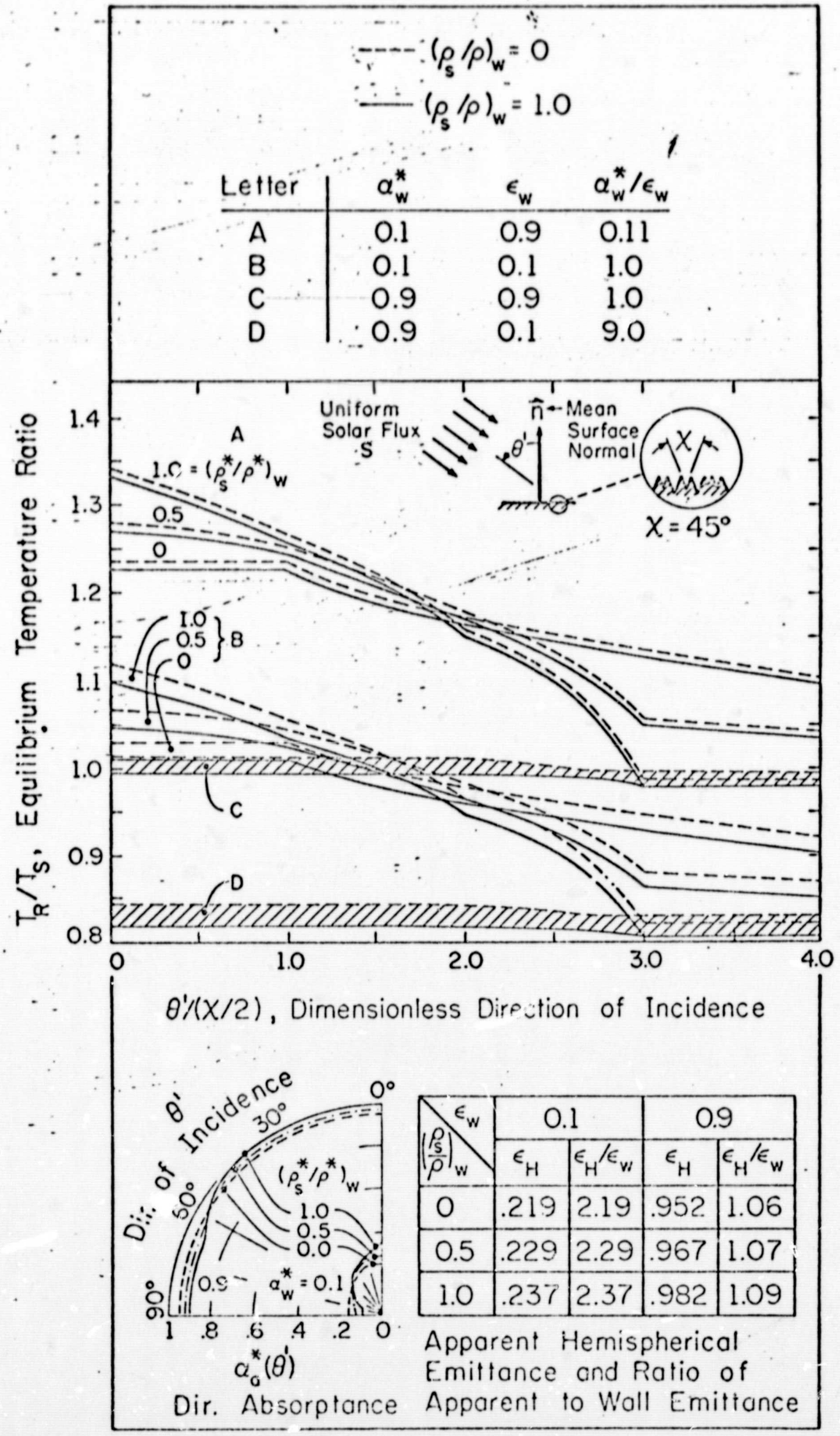

ϵ_w / $(\rho_s/\rho)_w$	0.1		0.9	
	ϵ_H	ϵ_H/ϵ_w	ϵ_H	ϵ_H/ϵ_w
0	.219	2.19	.952	1.06
0.5	.229	2.29	.967	1.07
1.0	.237	2.37	.982	1.09

Apparent Hemispherical Emittance and Ratio of Apparent to Wall Emittance

Figure 1. Surface roughness effects on equilibrium temperature (χ = 45°)

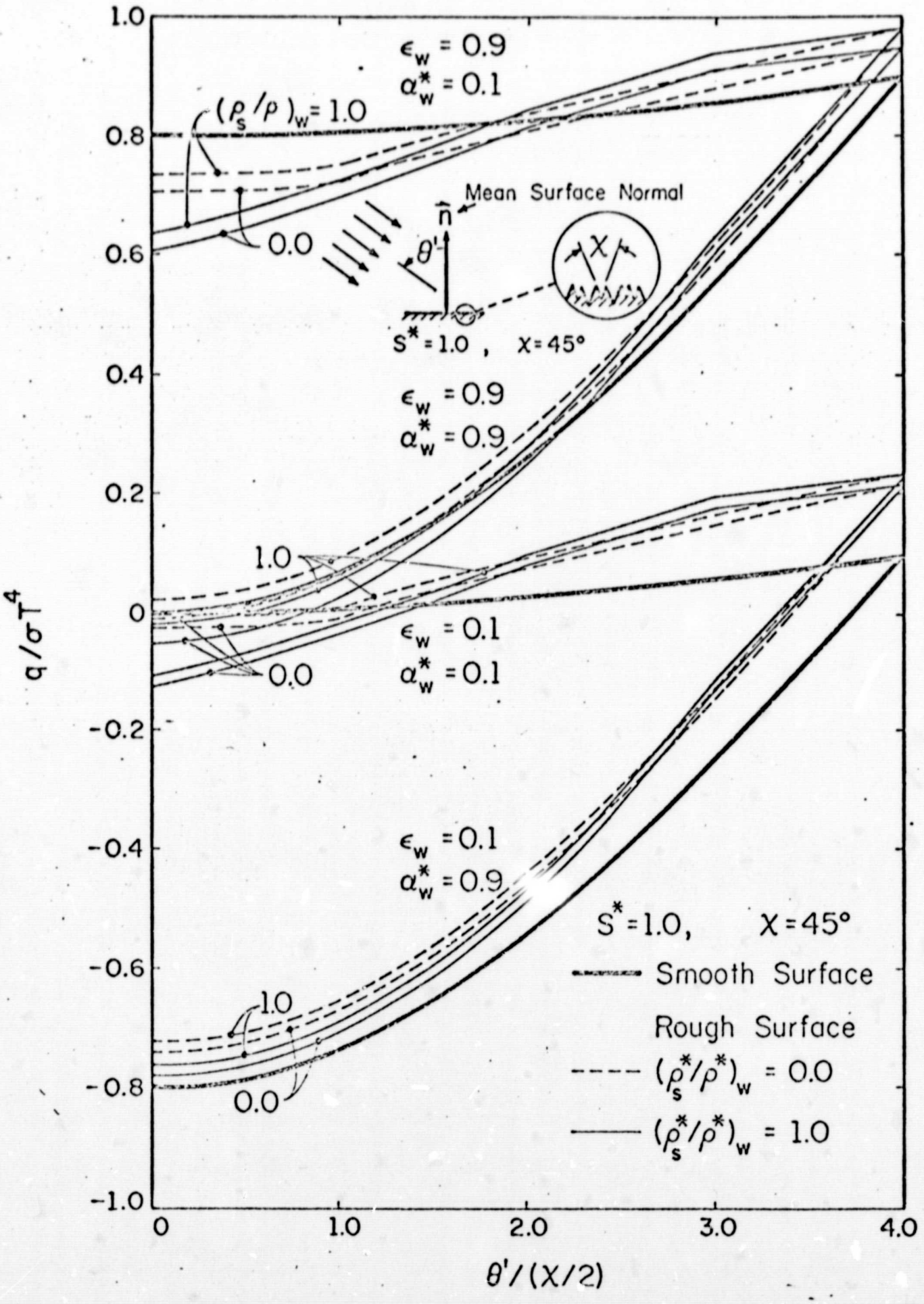

Figure 2. Surface roughness effects on radiant heat transfer ($S^* = 1.0$)

25

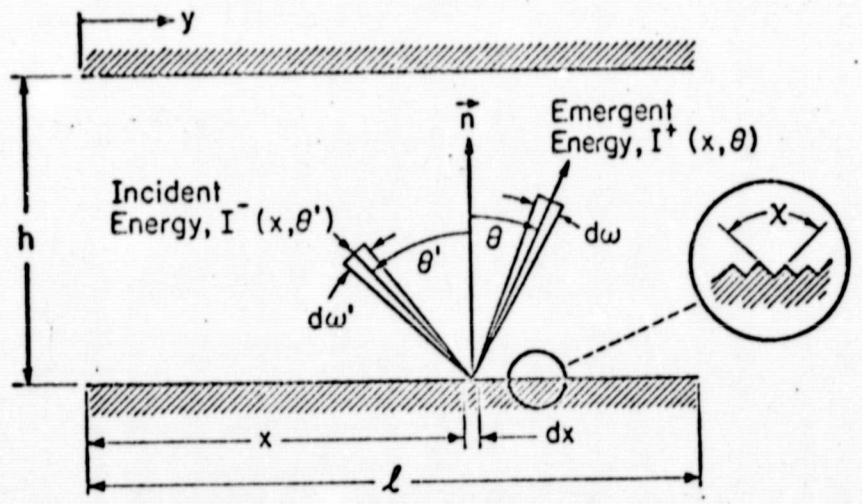

Figure 3. Schematic diagram of parallel plate system

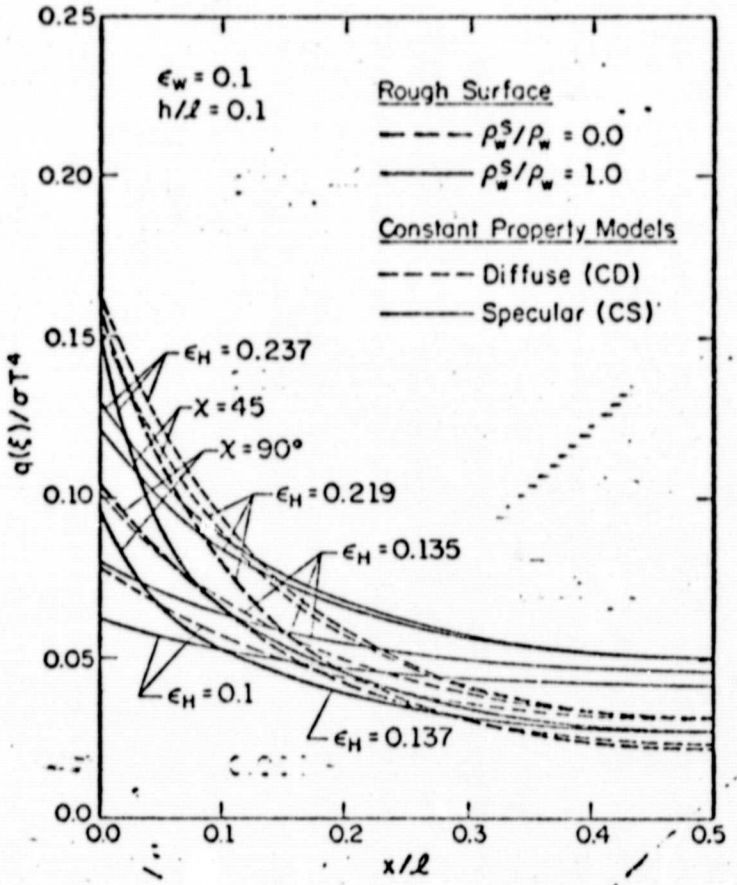

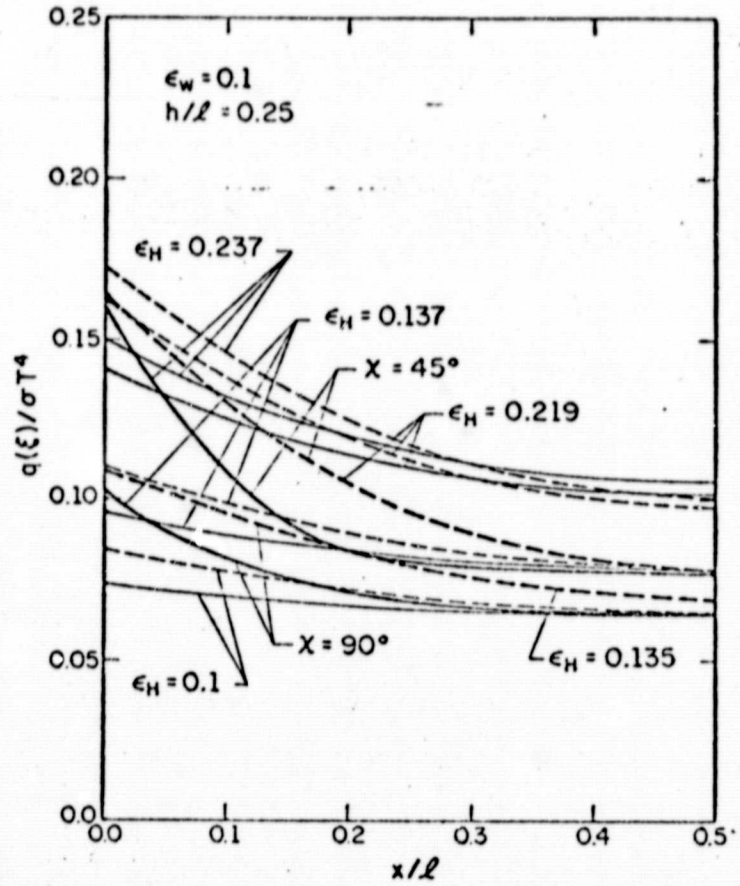

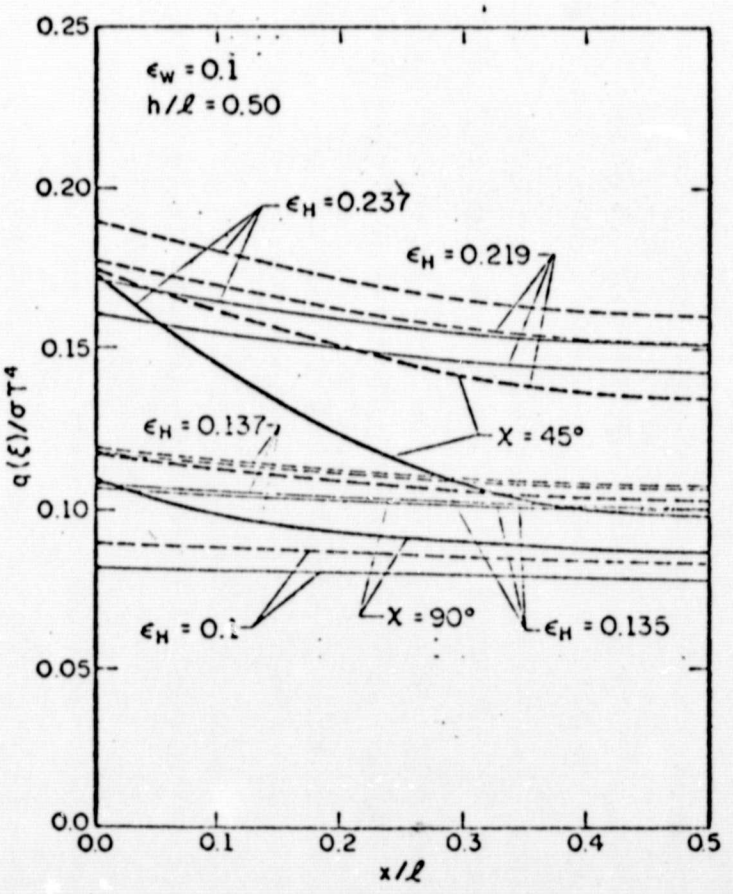

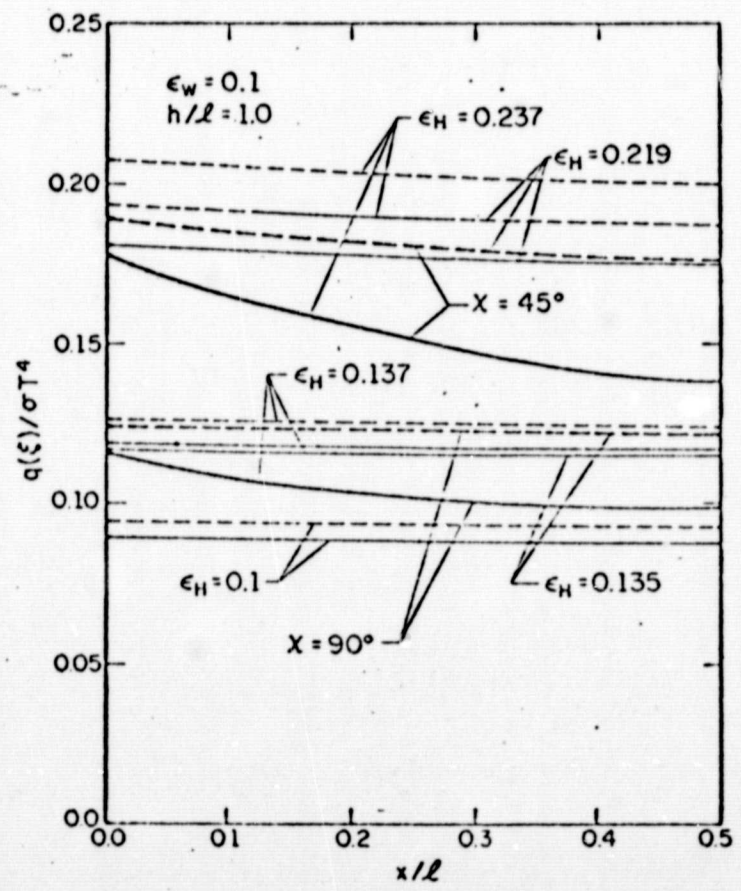

Figure 4. Comparison of dimensionless radiant flux distributions ($\epsilon_w = 0.1$)

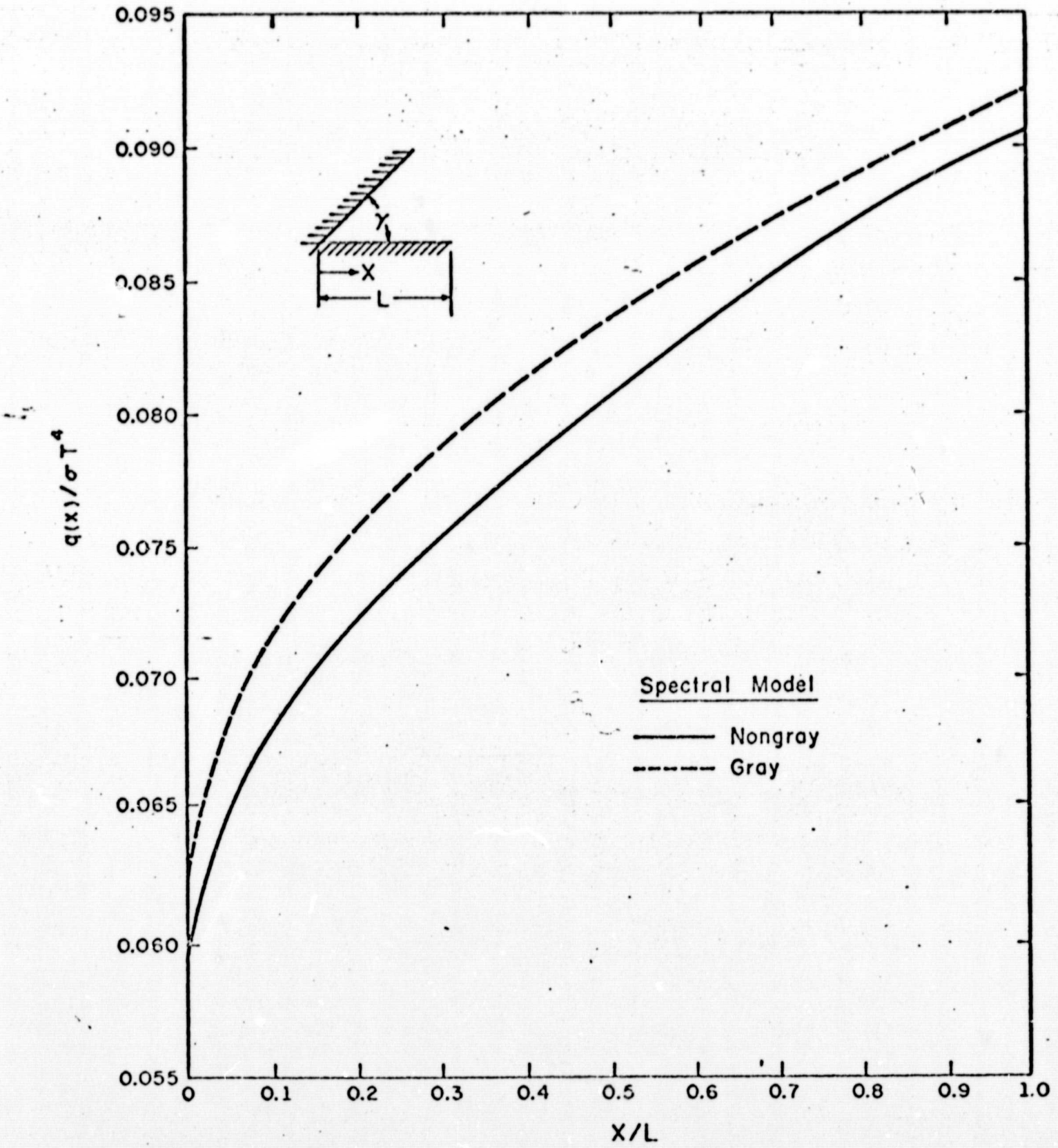

Figure 5. Comparison of dimensionless radiant flux distributions for equal temperature diffuse tungsten plates ($\gamma = 45°$, $T = 1980°R$)

28

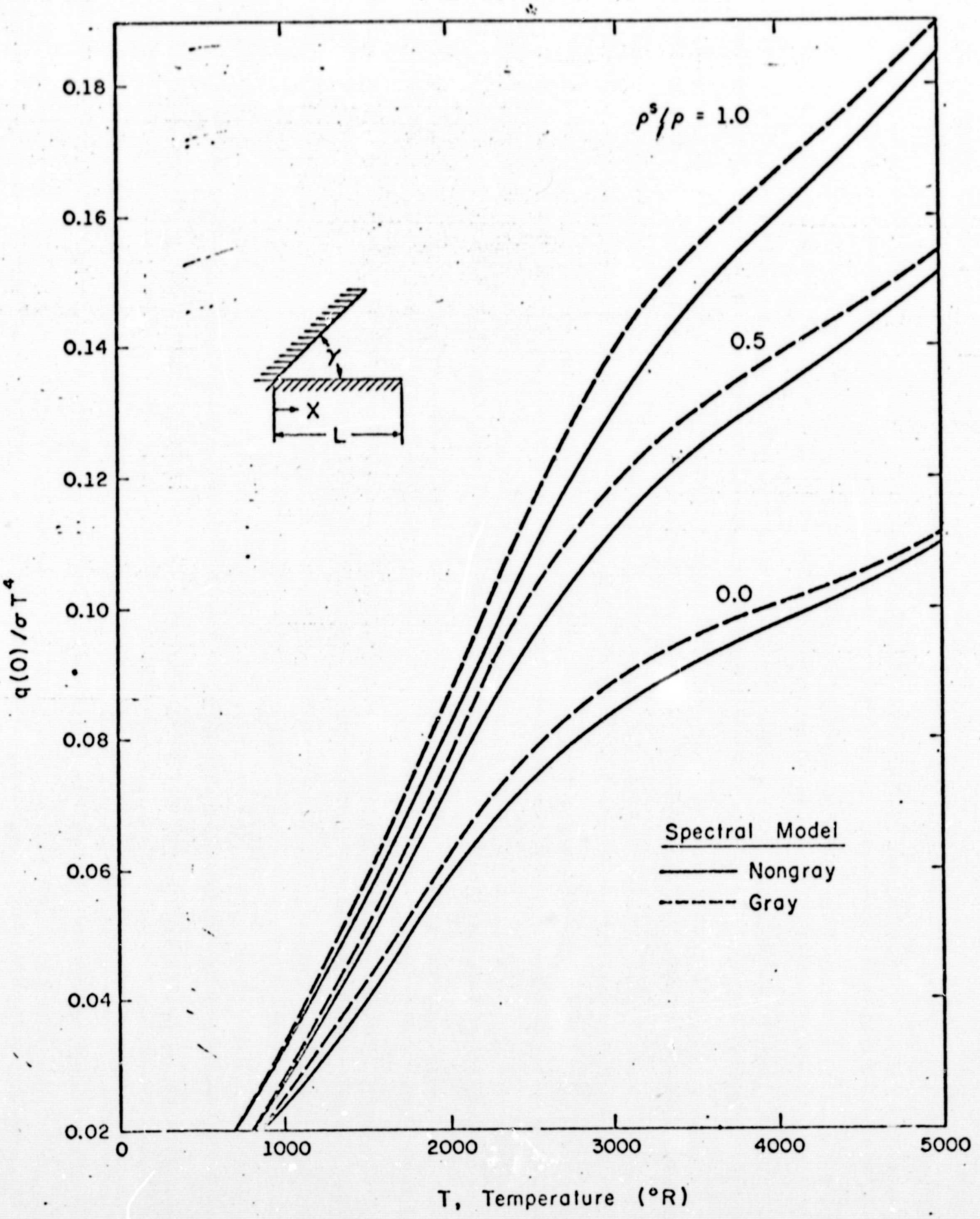

Figure 6. Comparison of nongray and gray dimensionless corner heat flux values for equal temperature tungsten plates ($\gamma = 45°$)

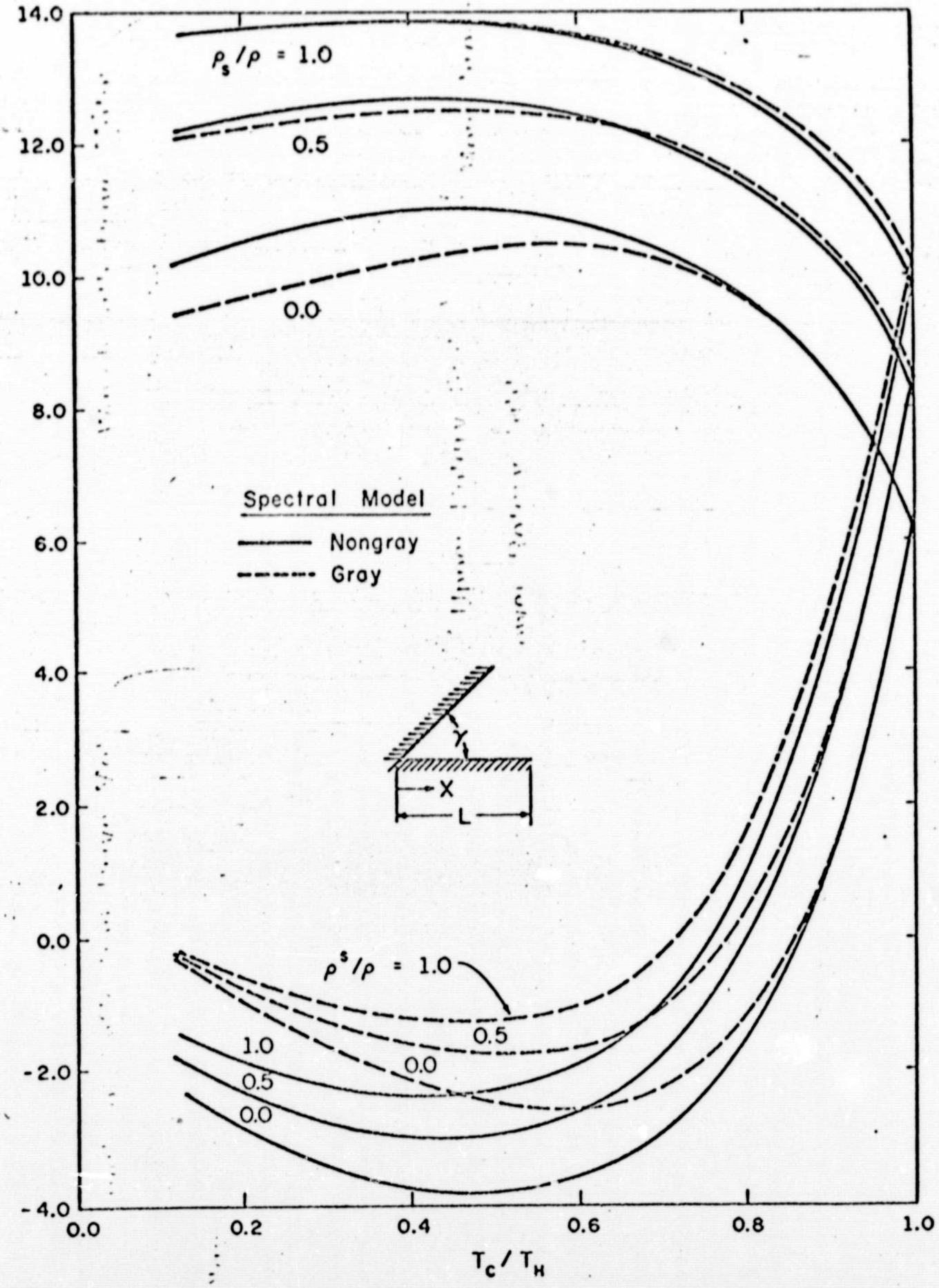

Figure 7. Comparison of nongray and gray corner heat flux values for unequal temperature tungsten plates ($\gamma = 45°$, $T_H = 4320°R$)

30

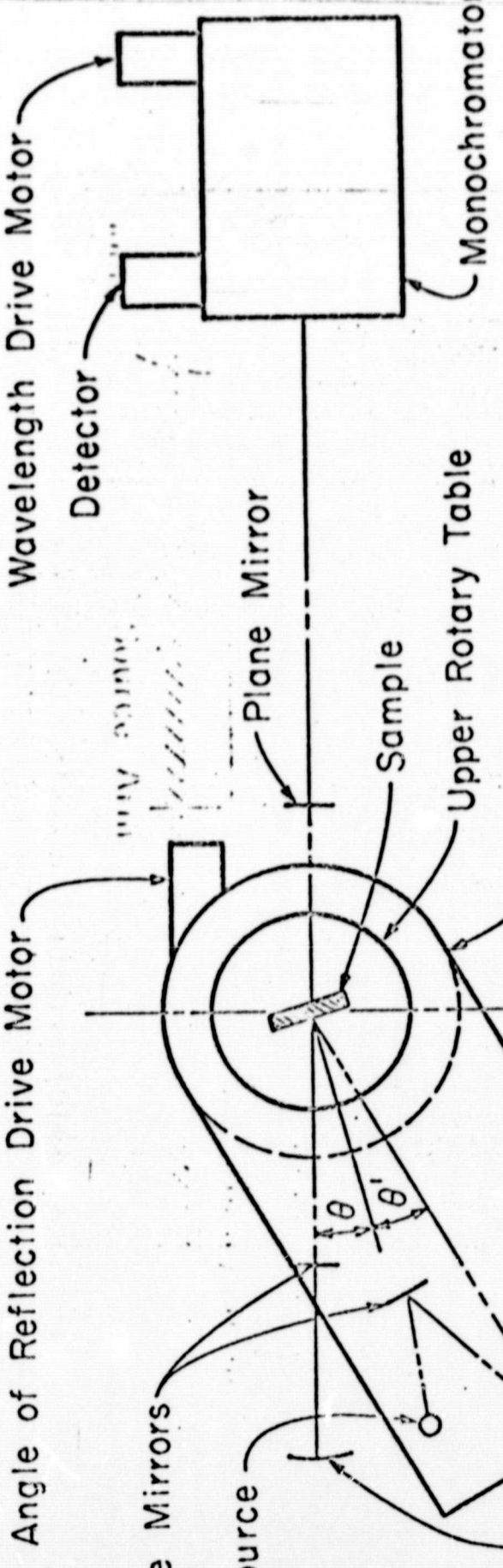

Figure 8. Schematic diagram of plane of incidence bidirectional reflectance measurement facility--top view

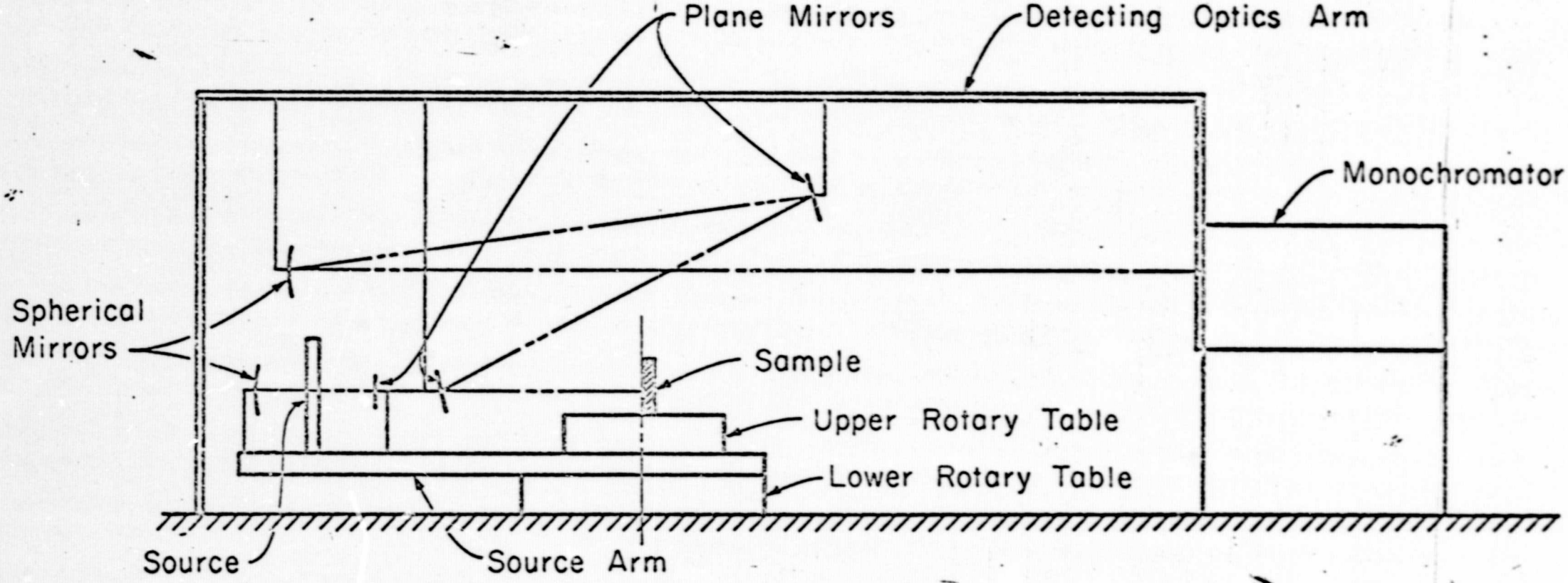

Figure 9. Schematic diagram of plane of incidence bidirectional reflectance measurement facility--side view

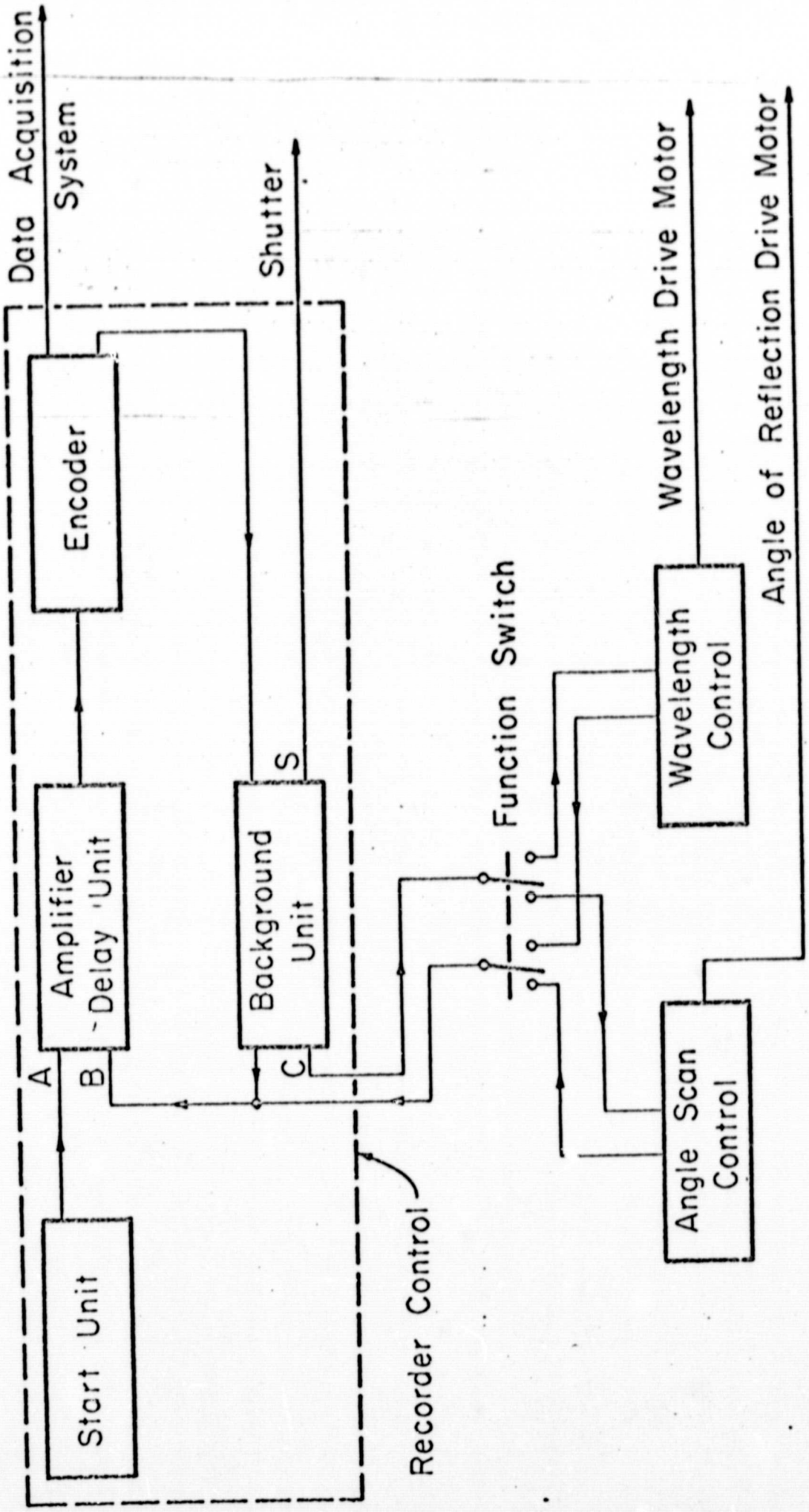

Figure 10. Schematic diagram of control system